FABRICATION, PHOTOCATALYTIC AND ADSORPTION OF IMMOBILIZED TiO_2/CHITOSAN-MONTMORILLONITE AND TiO_2/POLYANILINE BILAYER SYSTEMS FOR THE REMOVAL OF METHYL ORANGE DYE FROM AQUEOUS SOLUTIONS

NOOR NAZIHAH BINTI BAHRUDIN

UNIVERSITI SAINS MALAYSIA

2016

FABRICATION, PHOTOCATALYTIC AND ADSORPTION OF IMMOBILIZED TiO_2/CHITOSAN-MONTMORILLONITE AND TiO_2/POLYANILINE BILAYER SYSTEMS FOR THE REMOVAL OF METHYL ORANGE DYE FROM AQUEOUS SOLUTIONS

by

NOOR NAZIHAH BINTI BAHRUDIN

Thesis submitted in fulfillment of the requirements

for the degree of

Doctor of Philosophy

September 2016

ACKNOWLEDGEMENT

IN THE NAME OF ALLAH THE MOST GRACIOUS AND MOST MERCIFUL

First and foremost, all the praises and thanks are towards Allah, the Almighty, Who had given me strength, health and courage to complete this thesis. Special appreciation is dedicated to my research supervisor and mentor, Professor Dr Hj Mohd Asri Nawi who has been coaching me, especially in research from nothing till who I am today. Thank you, Prof, for your wise advice, patience, concern and constructive guidance throughout these years.

Special thanks are also awarded to Ministry of Higher Education of Malaysia for the sponsorship under My Phd program; FRGS grant; 203/PKIMIA/6711228 and Universiti Sains Malaysia for all the facilities provided. This thesis would not be completed without the help of these dedicated people; Mrs Nor Hayati, Mr Zamri, Mr Sujay, Mr Siva, Mr Johari, Ms Jamilah, Mrs Arlita, Mr Ong, Mr Yushamdan, SCS lecturers and supporting staff and to those whose names I didn't mention here, thanks a lot for your endless cooperation and patience during the period of my study. Special thanks are also forwarded to my amazing and inspiring colleagues; Dr Sumiyyah, Dr Wan Izhan, Dr Ali, Dr Lelifajri, Dr Sharin, Dr Karam, Dr Ngoh, soon to be Dr; Nazrina, Fathanah, Salmiah, Sheilatina, Norlizawati and Wan Siti Azahayu for their informative discussion and self-encouragement.

Last but not least, an endless appreciation is dedicated to my beloved family members, my father, Hj. Bahrudin Daud, my mother, Hjh. Maimunah Yunus, my sisters, Maisarah and Yuhanis for the everlasting love, support and encouragement through the thick and thin moments of my life. Hopefully, all the experiences, knowledge and practices that I gained throughout these years would make me a better person for myself, family, religion and nation, insya Allah.

TABLE OF CONTENTS

LIST OF TABLES

LIST OF FIGURES

LIST OF ABBREVIATIONS

1,4-BQ	1,4-benzoquinone
2,4-D	2,4-dichlorophenoxyacetic acid
AB1	acid black 1
APS	ammonium persulfate
BET	Brunauer-Emmet-Teller
BG	brilliant green
CS	chitosan
CS-MT/GP	chitosan-montmorillonite/glass plate single layer system
CR	Congo red
DMSO	dimethyl sulfoxide
EDX	energy dispersive X-Ray
ENR_{50}	epoxidized natural rubber of 50 % mole epoxidation
FTIR	Fourier transform infrared
GP	glass plate
HA	humic acid
HOMO	highest occupied molecular orbital
IUPAC	International Union of Pure and Applied Chemistry
LUMO	lowest occupied molecular orbital
MB	methylene blue
MG	malachite green
MO	methyl orange
MT	montmorillonite

PANI/ENR_{50}/PVC	polyaniline/epoxidized natural rubber/poly (vinyl) chloride
PANI/GP	polyaniline/glass plate single layer system
PL	photoluminescence
PVA-GLA	poly (vinyl) alcohol-glutaraldehyde
PVC	poly (vinyl) chloride
PVP	poly (vinyl) pyrrolidone
RB5	reactive black 5
SEM	scanning electron micrograph
TBOT	tetrabutyl orthotitanate
TiO_2/CS-MT/GP	titanium dioxide/chitosan-montmorillonite/glass plate bilayer system
TiO_2/GP	titanium dioxide/glass plate single layer system
TiO_2/PANI/GP	titanium dioxide/polyaniline/glass plate bilayer system
TOC	total organic carbon
UV-Vis DR	ultraviolet-visible diffuse reflectance
XRD	X-Ray diffraction

PEMFABRIKAN, FOTOMANGKINAN DAN PENJERAPAN SISTEM DWILAPISAN TERPEGUN TiO_2/KITOSAN-MONTMORILONIT DAN TiO_2/POLIANALINA UNTUK PENYINGKIRAN PEWARNA METIL JINGGA DARIPADA LARUTAN AKUEUS

ABSTRAK

Kajian ini adalah usaha untuk membangunkan dua sistem dwilapisan terpegun untuk penyingkiran secara fotomangkinan-penjerapan pewarna metil oren (MO) daripada larutan akueus. Sistem dwilapisan terpegun melibatkan penjerap spesifik dan TiO_2 di atas plat kaca yang dinamakan TiO_2/kitosan-montmorilonit (TiO_2/CS-MT/GP) dan TiO_2/polianalina (TiO_2/PANI/GP) masing-masing telah difabrikasi melalui teknik pelitupan celup. Dalam kajian ini, CS-MT dan PANI berfungsi sebagai lapisan bawah manakala fotomangkin TiO_2 dijadikan sebagai lapisan atas. Pada awalnya, lapisan bawah untuk kedua-dua sistem dioptimumkan melalui kajian penjerapan dan dicirikan melalui mikroskop imbasan elektron (SEM), spektroskopi transformasi inframerah Fourier (FT-IR) dan analisis penjerapan-penyahjerapan N_2. Penambahan serbuk MT kepada matrik CS menurunkan kadar pembengkakan, menambahkan kekuatan mekanikal dan luas permukaan (S_{BET}) daripada 3.82 kepada 4.38 $m^2\ g^{-1}$ manakala penambahan ENR_{50}-PVC menambahkan kekuatan mekanikal tetapi menurunkan S_{BET} serbuk PANI daripada 9.16 kepada 8.50 $m^2\ g^{-1}$. Penilaian aktiviti fotomangkinan oleh sistem dwilapisan dilakukan di bawah pancaran lampu pendarfluor kompak 45 Watt. Berat optimum lapisan penjerap adalah 1.27 dan 0.63 mg cm^{-2} untuk masing-masing TiO_2/CS-MT/GP dan TiO_2/PANI/GP manakala berat TiO_2 optimum untuk TiO_2/CS-MT/GP dan TiO_2/PANI/GP masing-masing adalah 2.54 dan 1.27 mg cm^{-2}. Sistem TiO_2/CS-

MT/GP dan TiO_2/PANI/GP masing-masing mematuhi model kinetik penjerapan pseudo tertib pertama Lagergren dan pseudo tertib kedua Ho dan Mc Kay. Model isoterma Freundlich pula berupaya untuk menerangkan mekanisma penjerapan pada keseimbangan dan pembauran intra-zarah adalah salah satu kadar penghad untuk kedua-dua sistem. Sistem dwilapisan menghasilkan lebih radikal $^{\cdot}OH$ daripada sistem monolapisan TiO_2 kerana kadar pemisahan pasangan elektron-lubang yang lebih baik manakala jurang tenaga jalur TiO_2 dikurangkan dari 3.02 eV kepada 2.94 dan 2.95 eV, masing-masing untuk sistem TiO_2/CS-MT/GP dan TiO_2/PANI/GP. Keadaan operasi optimum bagi aktiviti fotomangkinan-penjerapan sistem dwilapisan adalah pH ambien (6.5), kadar aliran udara 40 mL min^{-1} dan kepekatan awal MO 20 mg L^{-1}. Sistem TiO_2/CS-MT/GP boleh mengekalkan kebolehulangan guna dalam purata penyingkiran sebanyak 97.7 ± 1.0 % dan kadar penyingkiran 0.088 ± 0.008 min^{-1} sepanjang 10 kitaran manakala aktiviti fotomangkinan TiO_2/PANI/GP lebih baik pada tiga kitaran yang pertama tetapi mula menurun pada kitaran keempat dengan purata penyingkiran sebanyak 62.7 ± 10.2 % dan kadar penyingkiran adalah 0.017 ± 0.003 min^{-1}. Walau bagaimanapun, kadar penyingkiran sistem TiO_2/CS-MT/GP adalah 4 kali lebih baik dari TiO_2/GP manakala ia adalah 2.5 kali bagi sistem TiO_2/PANI/GP. Mineralisasi MO mencapai 82.8 % bagi TiO_2/CS-MT/GP dan 73.2 % bagi TiO_2/PANI/GP selepas 10 jam rawatan. Dalam pada itu, laluan penguraian menunjukkan spesis pertengahan utama yang terhasil adalah 4-{(E-[4-(metilamino)fenil]diazenil benzenasulfonat dan 4-{(E-[4-aminofenil]diazenil} benzenasulfonat. Secara perbandingan, sistem TiO_2/CS-MT/GP menunjukkan penyingkiran secara fotomangkinan-penjerapan pewarna MO yang lebih baik daripada sistem TiO_2/PANI/GP.

FABRICATION, PHOTOCATALYTIC AND ADSORPTION OF IMMOBILIZED TiO_2/CHITOSAN-MONTMORILLONITE AND TiO_2/POLYANILINE BILAYER SYSTEMS FOR THE REMOVAL OF METHYL ORANGE DYE FROM AQUEOUS SOLUTIONS

ABSTRACT

This study was an effort to develop two immobilized bilayer systems for the photocatalytic-adsorptive removal of methyl orange (MO) dye from aqueous solution. The immobilized bilayer systems involving specific adsorbents and TiO_2 on the glass plates namely TiO_2/chitosan-montmorillonite (TiO_2/CS-MT/GP) and TiO_2/polyaniline (TiO_2/PANI/GP) systems had been fabricated via a dip coating technique. In this study, CS-MT and PANI, respectively functioned as the sub-layer while TiO_2 photocatalyst was made as the top layer. Initially, the respective adsorbent sub-layer of both systems was optimized via a batch adsorption study and characterized by using scanning electron microscopy (SEM), Fourier transform infra-red spectroscopy (FT-IR) and N_2 adsorption-desorption analysis. The addition of MT powder to CS matrix decreased the swelling degree, improved the mechanical strength and surface area (S_{BET}) of CS-MT from 3.82 to 4.38 m^2 g^{-1} while the addition of ENR_{50}-PVC decreased the S_{BET} of PANI powder from 9.16 to 8.50 m^2 g^{-1} but improved its mechanical strength. The photocatalytic activity assessment of the bilayer systems was performed under the irradiation of a 45 Watts compact fluorescent lamp. The optimum adsorbent sub-layer loading was found to be 1.27 and 0.63 mg cm^{-2} for TiO_2/CS-MT/GP and TiO_2/PANI/GP, respectively, while the optimum TiO_2 loading for TiO_2/CS-MT/GP and TiO_2/PANI/GP was 2.54 and 1.27 mg cm^{-2}, respectively. The TiO_2/CS-MT/GP and TiO_2/PANI/GP systems obeyed the

Lagergren's pseudo first order and Ho and Mc Kay's pseudo second order adsorption kinetic model, respectively. On the other hand, the Freundlich isotherm model could explain the adsorption mechanism at equilibrium whereas intra-particle diffusion was one of the rate limiting steps for both systems. The bilayer systems produced more $^{\cdot}OH$ radicals than the single layer TiO_2 due to better charge separation rate of electron-hole pairs while the band gap of TiO_2 was reduced from 3.02 eV to 2.94 and 2.95 eV for TiO_2/CS-MT/GP and TiO_2/PANI/GP system, respectively. The optimum operating conditions for the photocatalytic-adsorption activity of the bilayer systems were at ambient pH (6.5), 40 mL min^{-1} of aeration flow rate and 20 mg L^{-1} of MO initial concentration. The TiO_2/CS-MT/GP could maintain the reusability on the average removal of 97.7 ± 1.0 % and 0.088 ± 0.008 min^{-1} removal rate throughout the 10 cycles, while the photocatalytic activity of TiO_2/PANI/GP was better at the first three cycles, but started to cease out at the 4^{th} cycle with the removal average of 62.7 ± 10.2 % and 0.017 ± 0.003 min^{-1} removal rate. Nevertheless, the removal rate of the MO of the TiO_2/CS-MT/GP system was 4 times better than TiO_2/GP while it was 2.5 times for the TiO_2/PANI/GP system. The mineralization of MO attained 82.8 % by TiO_2/CS-MT/GP and 73.2 % by TiO_2/PANI/GP after 10 hours of treatment. Meanwhile, the degradation pathways showed that the main intermediate species produced were 4-{(E-[4-(methylamino)phenyl] diazenyl}benzenesulfonate and 4-{(E-[4-aminophenyl] diazenyl}benzenesulfonate. Comparatively, the TiO_2/CS-MT/GP system showed better photocatalytic-adsorptive removal of the MO dye than the TiO_2/PANI/GP system.

CHAPTER ONE

INTRODUCTION

1.1 Photocatalysis: Historical Overview

Photocatalysis is defined as a photoreaction in the presence of a catalyst. This photoreaction is activated by photons from the light by appropriate energy (Mills and Le Hunte, 1997). According to Fujishima *et al*. (2008), the earlier work of photocatalysis had been reported by Renz at University of Lugano whereby he discovered that titania is partially reduced during the illumination of light in the presence of an organic compound, in which the oxide turns to dark colors (gray, blue and black) (Renz, 1921). Then, in 1924, Baur and Perret at the Swiss Federal Institute of Technology reported the photocatalytic deposition of metallic silver by ZnO. The studies were then continued for more years by different scientists and the progressed of those studies are shown in time frame as in Figure 1.1.

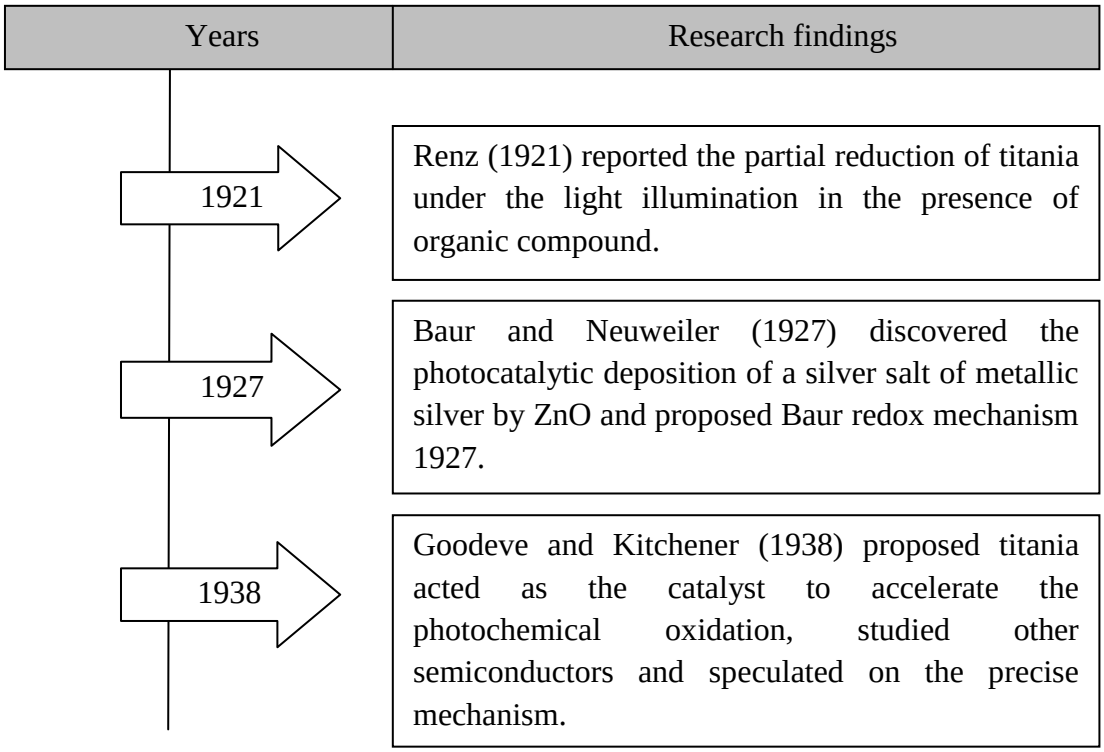

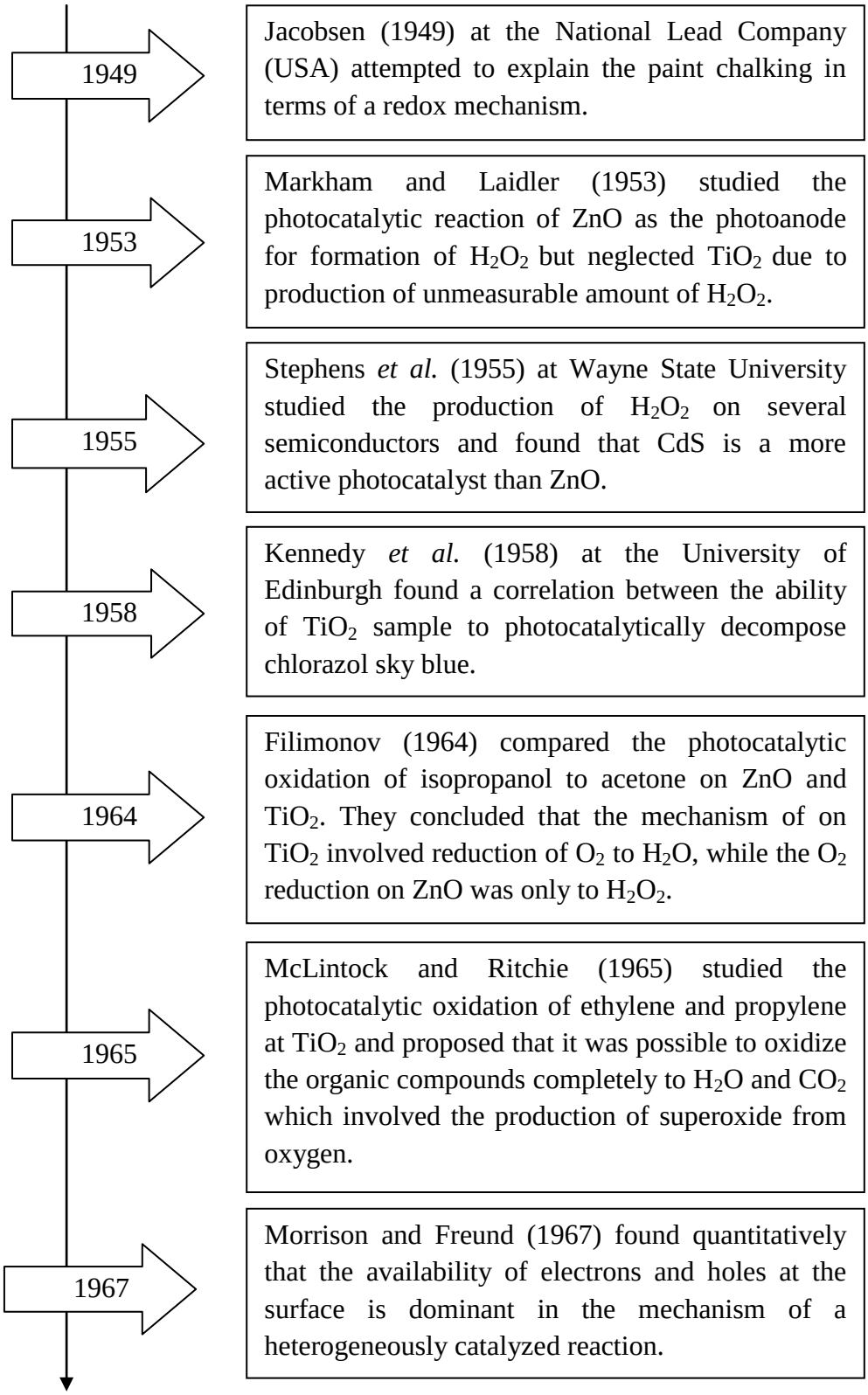

Figure 1.1: Time frame of photocatalysis research progress (Fujishima *et al*., 2008).

The historical breakthrough of photocatalysis was catalyzed by the demand of energy renewal and storage and the detoxification of harmful substances in water and air especially in the late 1960s (Ibhadon and Fitzpatrick, 2013; Linsebigler *et al*., 1995). In 1972, Akira Fujishima and his doctoral advisor, Kenichi Honda discovered the splitting of water by TiO_2 electrode in an electrochemical cell after an exposure to light of 415 nm wavelength (Fujishima and Honda, 1972). In the experiment (Figure 1.2), the photocurrent flowed from Pt counter electrode through the external circuit to TiO_2 electrode which was proven to cause the oxidation of water at the TiO_2 electrode with the evolution of oxygen while it was the reduction of water at the Pt electrode with the evolution of hydrogen (Nakata *et al*., 2012). Since then, there has been a growing interest in this discovery (oxidation and reduction potential of TiO_2) for numerous applications such as water splitting, hydrogen production, electrode and water/air treatment especially in the field of heterogeneous photocatalysis.

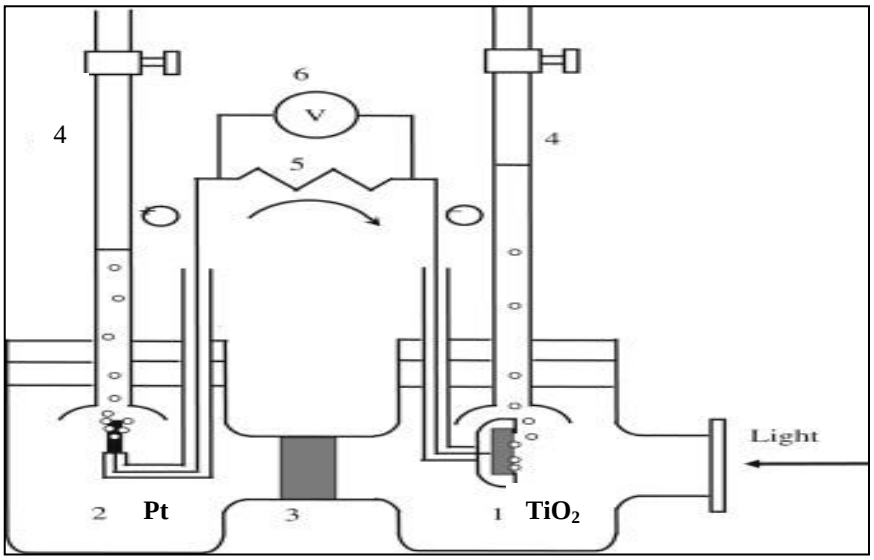

Figure 1.2: Schematic diagram of electrochemical photocell. (1) n-type TiO_2 electrode; (2) platinum black counter electrode; (3) ionically conducting separator; (4) gas buret; (5) load resistance; and (6) voltmeter (Hashimoto *et al.*, 2005).

1.2 Heterogeneous photocatalysis

Application of photocatalysis is generally divided into homogeneous and heterogeneous photocatalysis. The homogeneous photocatalysis generally refers to the reactants and the photocatalysts existing in the same phase while the heterogeneous photocatalysis refers to photoreaction of a catalyst which is in a different phase from the reactants. Common examples of homogeneous photocatalysis are ozonation and photo-Fenton systems (Fe^{2+} and Fe^{2+}/H_2O_2) (Kitsiou *et al.*, 2009). Heterogeneous photocatalysis includes the process involving light irradiation on semiconductors namely TiO_2, ZnO, ZnS and CdS. Examples of heterogeneous photocatalysis are mild/total oxidation, dehydrogenation, hydrogen transfer, deuterium-alkane isotopic exchange, metal deposition, water detoxification and gaseous pollutant removal (Herrmann, 1999). The basic components of heterogeneous photocatalysis are (Teh and Mohamed, 2011);

1) An emitted photon of appropriate wavelength,
2) a strong oxidizing agent (O_2) and
3) a catalyst surface of a semiconductor material.

A semiconductor can be a material with electrical resistivity between that of an insulator and a conductor while a semiconductor photocatalyst is characterized by an electronic band structure in which the highest occupied energy band, valence band (VB) and conduction band (CB) are separated by a band gap (E_{bg}). The CB is the energy level for the reduction potential of photoelectrons; VB is for the oxidizing ability of photogenerated holes while the band gap defines the wavelength sensitivity of the semiconductor to irradiation. The magnitude of the fixed energy gap between the electron rich valence band and the largely vacant conduction band governs the extent of the thermal population of the conduction band (Fox and Dulay, 1993). In

other words, the higher band gap of a semiconductor corresponds to shorter light wavelength which eventually requires a higher energy for electron excitation from the VB to CB. However, the electronic band of a semiconductor is often confused with the electronic band of a dye molecule. The difference between the energy level in a semiconductor photocatalyst and a dye molecule is shown in Figure 1.3.

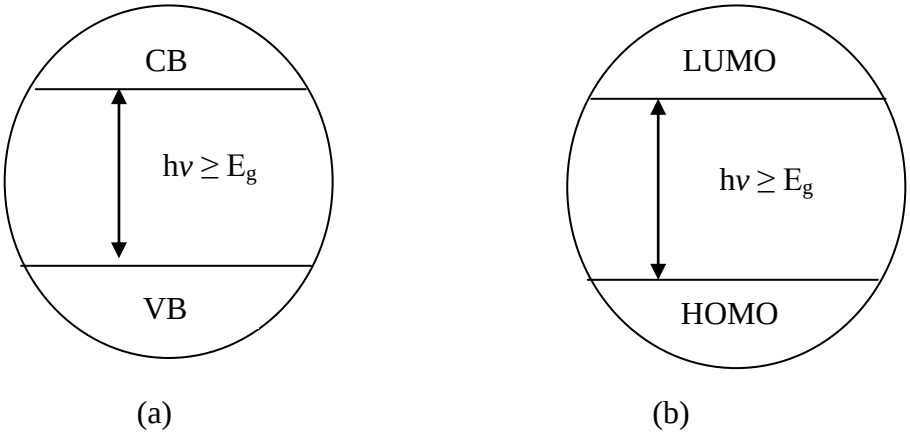

Figure 1.3: The energy level diagram of a) a semiconductor and b) a dye molecule.

According to Pankaj *et al*. (2013), a semiconductor must be non-toxic, stable in aqueous solution containing toxic or reactive chemicals and resistant to photocorrosion under sunlight. Numerous semiconductors have been tested for heterogeneous photocatalysis especially for the purpose of environmental remediation such as ZnO, ZnS and CdS. Unfortunately, these semiconductors suffer from photocorrosion in which the former photocatalyst (ZnO and ZnS) releases $Zn(OH)_2$ and Zn^{2+} while the latter (CdS) releases Cd^{2+} ions upon irradiation in aqueous media (Pankaj *et al*., 2013). Titanium dioxide (TiO_2) on the other hand, possesses several important characteristics such as stable, non-toxic, and inert and is now considered an effective photocatalyst (Mills *et al*., 2015).

1.3 Titanium dioxide

1.3.1 Ideal photocatalyst

The successful application of TiO_2 in water purification was firstly reported in 1977 (Frank and Bard, 1977) on cyanide and sulfite. The specialty of TiO_2 which made it differs from other photocatalyst is in mixings of both of its anatase and rutile forms (Li *et al*., 2006). With the attractive and successful degradation of many organic pollutants, TiO_2 has become the most chosen photocatalyst in the field of photocatalysis. Table 1.1 lists the characteristics of TiO_2 which closely matches the ideal photocatalyst characteristics.

Table 1.1: The characteristics match of ideal and TiO_2 photocatalyst (Hondow *et al*., 2010; Ibhadon and Fitzpatrick, 2013).

Ideal photocatalyst	TiO_2	Remarks
Photoactive	√	High photoactivity in the presence of light.
Able to absorb visible and/or near UV light		Only active for light irradiation of wavelength $\lambda \leq 387$ nm however, it can be modified to adsorb light of $\lambda \geq 387$ nm.
Biologically and chemically inert	√	Does not take part in the reaction whereby only acting as the mediator for redox reactions.
Photostable (not liable to photoanonic corrosion)	√	Practical for long term use and applications
Inexpensive	√	Naturally abundant resource of titanium
Non-toxic	√	Safe for human and environment
Able to oxidize and reduce water to O_2 and H_2, respectively	√	The photogenerated electron-holes can react with water via redox reaction to produce O_2 and H_2 since the band is larger than 1.23 eV.

1.3.2 Structure and properties

TiO_2 is a metal oxide with a molar mass of 79.90 g mol^{-1} and classified as not hazardous by the United Nations (UN) Globally Harmonized System (GHS) of Classification and Labeling of Chemicals (IARC, 2010). The photocatalytic activity of TiO_2 is highly dependent on the geometry, crystalline phases, surface defects, specific surface area and particle sizes (Dai *et al*., 2015). There are three types of TiO_2 phase that are mostly studied; rutile, anatase and brookite as shown in Figure 1.4. Rutile is the most stable phase of TiO_2, followed by anatase and brookite which are metastable and can be transformed to rutile when heated (Kaplan *et al*., 2015). Other type of TiO_2 polymorphs namely TiO_2(B) and the layered titanates are rarely studied. However, the anatase has been reported to exhibit the best photoactivity among the three phases due to its efficiency in light harvesting, prolong the lifetimes of charge carriers and charge separation (Kaplan *et al*., 2015; Leyva *et al*., 2015). On the other hand, rutile phase suffers the weaker adsorption of organic pollutants and faster recombination of electron-hole pairs while brookite is difficult to synthesize (Zhang *et al*., 2011). In recent years, the preparation of mixed phase TiO_2 is actively being studied such as anatase-rutile (Wu *et al*., 2015; Zhang *et al*., 2015b; Zhang *et al*., 2015), anatase-TiO_2(B) (Dai *et al*., 2015; Parayil *et al*., 2013), and anatase-brookite (Zhang *et al*., 2011).

The commercial mixed phase TiO_2 (anatase and rutile) is currently available in the market, namely Millenium 1580 S, Kronos 7500 and Kronos 1002 and Evonik P-25 or Aeroxide P25 (Montes *et al*., 2014). Aeroxide P-25 TiO_2, which was used in this study, consists of 80 % of anatase and 20 % of rutile. According to the product information from Evonik, P-25 TiO_2 has a surface area of 50 ± 15 m^2 g^{-1} and average particle size of 21 nm. The mixture of anatase and rutile in P-25 TiO_2, enhances the

photoactivity due to low recombination of electron-hole pairs as a result of relative conduction band edge between the anatase and rutile (Dai *et al*., 2015). P-25 TiO_2 has become the standard photocatalyst among the other brand of TiO_2 as it exhibits good photoactivity for the degradation of varieties of pollutants whereby it became the main reason of the selection for this study.

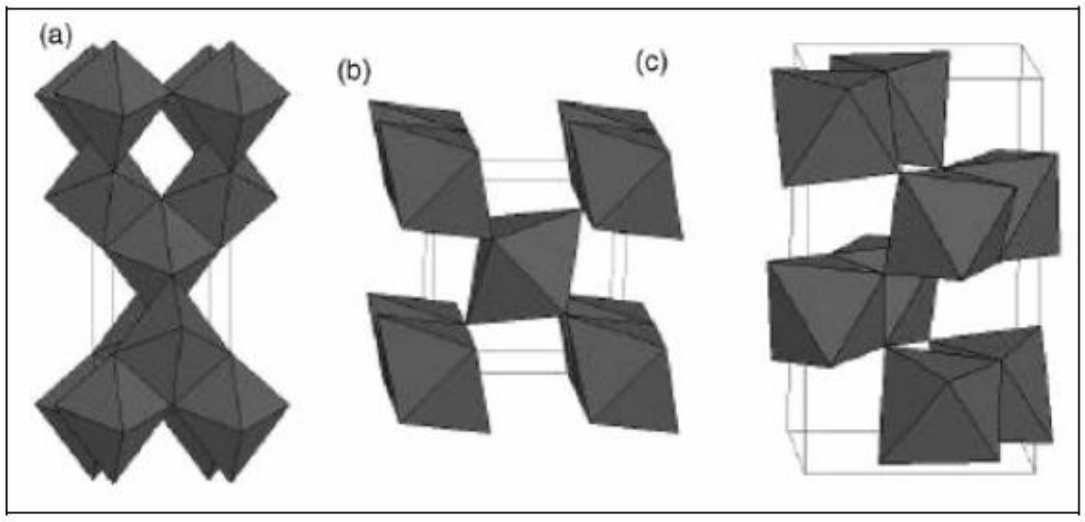

Figure 1.4: The crystal structures of TiO_2; (a) anatase, (b) rutile and (c) brookite (Leandro *et al*., 2013).

1.3.3 Mechanism of the TiO_2 photocatalysis

The process of photocatalysis is initiated when light of appropriate wavelength was absorbed by TiO_2 photocatalyst. According to physic's law, the wavelength is inversely proportional to the band gap energy. Therefore, the light wavelength should be similar or less than 380 nm since the band gap energy should be similar or greater than the band gap of TiO_2 for electron excitation from the valence to the conduction band to occur. The reaction on TiO_2 is shown as follows (Singh *et al.*, 2013; Zangeneh *et al.*, 2015):

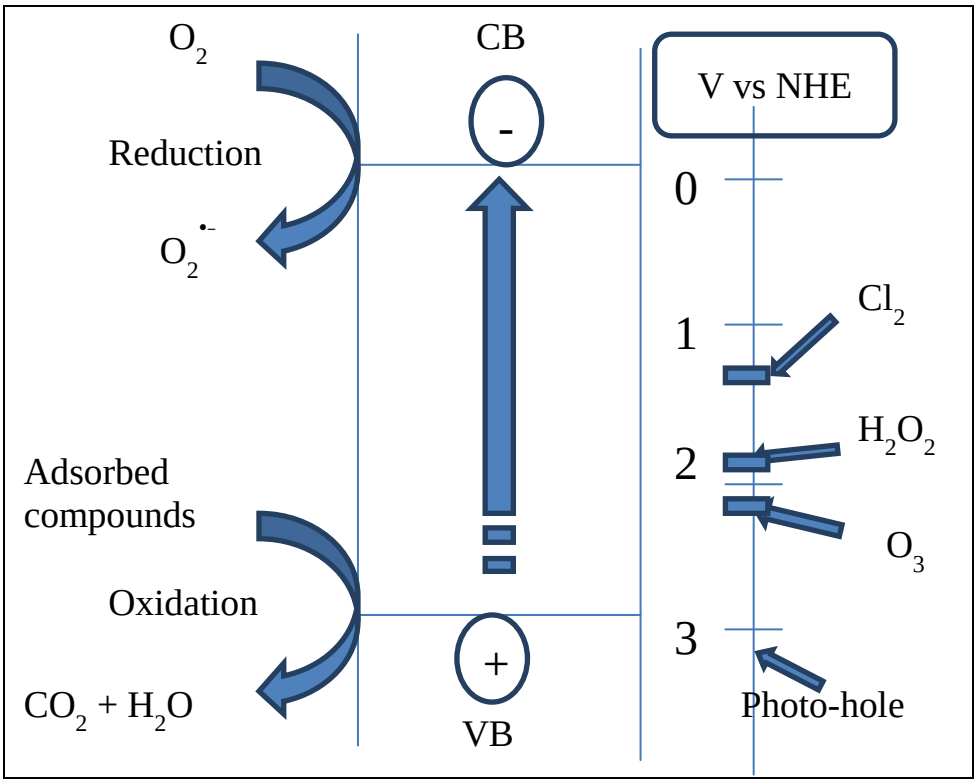

Figure 1.5: Schematic energy diagram of TiO_2 as adapted from Kazuhito *et al.* (2005).

Step 1: Generation of photoholes and electrons:

$$TiO_2 + hv \longrightarrow TiO_2 (e^-_{CB}) + TiO_2 (h^+_{VB}) \quad (1.1)$$

Step 2: Formation of hydroxyl radicals ($^{\bullet}OH$) by the photogenerated holes at valence band:

$$H_2O + h^+_{VB} \longrightarrow H^+ + {}^{\bullet}OH \quad (1.2)$$

$$OH^- + h^+_{VB} \longrightarrow {}^{\bullet}OH \quad (1.3)$$

Step 3: Formation of superoxide anion radical ($O_2^{\bullet -}$), hydroperoxyl radical ($^{\bullet}OOH$), hydrogen peroxide (H_2O_2) and hydroxyl radicals at the conduction band:

$$O_2 + e^-_{CB} \longrightarrow O_2^{\bullet -} \quad (1.4)$$

$$O_2^{\bullet -} + H^+ \longrightarrow {}^{\bullet}OOH \quad (1.5)$$

$${}^{\bullet}OOH + {}^{\bullet}OOH \longrightarrow H_2O_2 + O_2 \quad (1.6)$$

$$H_2O_2 + e^-_{CB} \longrightarrow OH^- + {}^{\bullet}OH \quad (1.7)$$

$$H_2O_2 + O_2^{\bullet -} \longrightarrow {}^{\bullet}OH + OH^- + O_2 \quad (1.8)$$

Step 4: Oxidation of organic contaminant (R):

$$R + {}^{\bullet}OH \rightarrow \rightarrow \rightarrow CO_2 + H_2O \quad (1.9)$$

$$R + O_2^{\bullet -} \rightarrow \rightarrow \rightarrow CO_2 + H_2O \quad (1.10)$$

$$R + h^+_{VB} \rightarrow R^{\bullet +} \rightarrow \text{the degradation products} \quad (1.11)$$

$$R + e^-_{CB} \rightarrow R^{\bullet -} \rightarrow \text{the degradation products} \quad (1.12)$$

A successful photocatalytic oxidation of organic pollutants by TiO_2 is highly dependent on the production of ${}^{\bullet}OH$ radicals at the VB of TiO_2. However, the generated ${}^{\bullet}OH$ radical is unstable and must be continuously generated *in situ*, by chemical or photochemical process (Leandro *et al*., 2013). Unless there are electron acceptors at the CB of TiO_2 after the excitation, the excited electrons could recombine with the photogenerated holes at the VB. Moreover, the recombination of electron-hole pairs would produce heat, which is unfavorable for the efficacy of the photocatalyst activity.

1.3.4 Langmuir-Hinshelwood kinetic model

The Langmuir Hinshelwood equation was commonly used as to describe the heterogeneous photocatalysis. The equation of the Langmuir Hinshelwood kinetic model is given as in Equation 1.13 (Kumar *et al.*, 2008a).

$$r = -\frac{dC}{dt} = \frac{k_r KC}{1 + KC'} \quad (1.13)$$

where r is the rate of reaction that changes with time.

The term r in Equation 1.13 was represented in terms of initial reaction rate, r_o, as a function of the initial dye concentration, C_o, or in terms of C_e, where C_e is the equilibrium dye concentration in solution. The initial rate of reaction as a function of C_o and C_e is given by Equations 1.14 and 1.15, respectively:

$$r_o = \frac{k_r K C_o}{1 + K C_o} \tag{1.14}$$

$$r_o = \frac{k_r K C_e}{1 + K C_e} \tag{1.15}$$

The parameter k_r and K which is a function of C_o or C_e can be predicted by linearizing Equations 1.14 and 1.15 as follows:

$$\frac{1}{r_o} = \frac{1}{k_r} + \frac{1}{k_r K C_o} \tag{1.16}$$

The constants k_r and K can be calculated from the corresponding integrated expression between the limits: $C = C_o$ at $t = 0$ and $C = C_t$ at $t = t$. The integrated expression is given by:

$$\ln\left(\frac{C_o}{C_t}\right) + K (C_o - C) = k_r K t \tag{1.17}$$

If the term $KC << 1$, the equation (1.13) is reduced to:

$$r = -\frac{dC}{dt} = k_r K C \tag{1.18}$$

Integrating equation (1.18) with respect to limits: $C = C_o$ at $t = 0$ and $C = C_t$ at $t = t$, the Langmuir Hinshelwood expression reduces to a pseudo first order kinetic and is given by:

$$\ln\left(\frac{C_o}{C_t}\right) = k_r K t = kt \tag{1.19}$$

where the new constant k includes k_r and K.

A plot of $\ln\left(\frac{C_o}{C_t}\right)$ versus time (t) will give a straight line with the slope of k as the pseudo first order rate constant. The coefficient of determination (R^2) indicates the degree of agreement of the reaction with the Langmuir-Hinshelwood kinetic model, where;

r: the rate of degradation (mg L^{-1} min);

C_e: the equilibrium concentration of pollutant (mg L^{-1});

C_o: the initial concentration of pollutant (mg L^{-1});

C_t: the concentration of pollutant at time t during degradation (mg L^{-1});

K: equilibrium constant for adsorption of the substrate onto catalyst;

k_r: limiting rate constant of reaction at maximum coverage under the given experimental conditions;

r_o: initial rate of reaction (min^{-1});

t: the irradiation time (min);

k: the reaction rate constant (min^{-1}).

1.3.5 Drawbacks and improvements

Though many researchers had reported the excellent performance by TiO_2 photocatalyst in water abatement, it suffers from several drawbacks such as high recombination rate of electron-hole pairs and poor degradation rate for some organic pollutants. Therefore, the research progress in photocatalysis field continues to grow and new methods are being developed in order to overcome those obstacles.

The first intrinsic problem with TiO_2 photocatalyst was its high recombination rate of electron-hole pairs upon light irradiation. It was known that the lifetime of charge carriers in TiO_2 after excitation was very short which is 10-40 μs

(Colbeau *et al*., 2003). The short lifetime due to high recombination of charge carriers could be overcome by surface sensitization using dye or metal complexes in order to induce better charge separation. The dye is anchored on TiO_2 surface by covalent, or physical or chemical bonding which induced the charge injection of the excited dye molecule into the CB of TiO_2 leading to successive photocatalytic degradation. This sensitization also increases the range of wavelength response towards the natural sunlight (Gupta and Tripathi, 2011). However, the dyes themselves can be photodegraded to form intermediates which need to be disposed. On the other hand, transition metal complexes such as Ru-polypyridyl complexes induce the charge separation by the excited electrons which participate in the charge transfer of electrons to TiO_2 conduction band (Kalyanasundaram and Grätzel, 1998).

The second drawback of TiO_2 is the excitation of electron-hole pairs could be only initiated in the presence of high UV light intensity. Therefore, the solution is to change the band gap energy by coupling two semiconductors of suitable potential energy such as CdS-TiO_2, SnO_2-TiO_2 and ZnO-TiO_2 whereby the holes produced in smaller band gap semiconductor remain while the electrons are transferred to the conduction band of TiO_2 which induce charge separation (Jing and Guo, 2006). Another way is to dope TiO_2 with noble metals such as Ag (Albiter *et al*., 2015; Gomathi and Mohan, 2010), Au (Subramanian *et al*., 2003; Tahir *et al*., 2006; Zhu *et al*., 2009), Pt, Ni, Rh and Cu (Gupta and Tripathi, 2011) which can trap the electrons and free holes and enhance the charge separation at the valence band to participate in the photocatalytic oxidation reaction. This was due to the Fermi levels of these noble metals which are lower than that of TiO_2. Nevertheless, it was found that the properties of these TiO_2-noble metal composites are strongly dependent on the size of metal particle, composition and dispersion as if the concentration of metal was too

high, the absorption of the light photon would be reduced and the metal can become the electron-hole recombination centers which resulted in lower efficiency than the TiO_2. TiO_2 can also be doped with non-metal such as C,N,B,F (Valentin and Pacchioni, 2013) and carbon nano tube (CNT) (Ashkarran *et al*., 2015). The composites could decrease the band gap which make it visible light active. In addition, the TiO_2 could be also modified by co-doping the metal-metal such as Fe^{3+} and Eu^{3+} (Vasiliu *et al*., 2009), metal-non-metal; Cu-N (Song *et al*., 2008) and non-metal-non-metal; C-N (Nawawi and Nawi, 2014; Sabri *et al*., 2015). The TiO_2 co-doped system showed a red-shift in absorption spectrum and high photocatalytic activity than the single doped TiO_2 especially when exposed to total visible light.

Thirdly, the conventional TiO_2 in suspended or slurry mode requires post treatment due to its nanoparticle size, which is a tedious, time and money consuming filtration process. Apart from filtration, the steps of recovering the photocatalyst from the treated water solution involved the process of washing, filtering and drying, which may result in the lost of an amount of the photocatalyst during the process. To solve this drawback, different supports and immobilization techniques were used whereby the common support materials and their immobilization modes were glass beads; heat attachment (Daneshvar *et al*., 2005), granular activated carbon; dip hydrothermal (Wang *et al*., 2009), stainless steel; coating (Souzanchi *et al*., 2013) and glass plate; dip coating (Razak *et al*., 2014). However, the immobilization mode of TiO_2 might have some significant defects such as reducing the active sites exposure to light, as the area is fixed and the mass transfer hindrance increases, which lead to poor photocatalytic activity plus the need to seek for well-defined procedures and equipment (Singh *et al*., 2013). Coupling the photocatalyst and adsorbent in the immobilized form is another approach to enhance the overall

photocatalytic performance. TiO_2 has been combined with various adsorbents such as silica oxide (SiO_2) (Rahman *et al*., 2014), montmorillonite (MT) (Bhattacharyya *et al*., 2004), activated carbon (AC) (Muthirulan *et al*., 2013) and chitosan (CS) nanofiber (Razzaz *et al*., 2016) whereby all systems showed enhanced photocatalytic performance than the bare TiO_2 in the removal of the organic contaminants.

1.4 Chitosan (CS)

1.4.1 Origin of CS

Chitin is firstly identified in 1884 and is originated from the main component on shell of crustaceans such as shrimp and crab shell and cell walls of fungi and yeast (Younes and Rinaudo, 2015). Chitin was the second most abundant polysaccharides in nature after cellulose while CS is the derivation of chitin which had undergone the deacetylation process using NaOH as the deacetylation agent (Choi *et al*., 2016). Figure 1.6 provides the chemical structures of cellulose, chitin and CS. Chitin with more than 75 % degree of deacetylation is known as CS while cellulose only differs with chitin and CS based on the hydroxyl group in its C-2 position. The process of deacetylation removes acetyl groups from the molecular chain of chitin and leaving behind a complete amino group ($-NH_2$). The degree of deacetylation depends on the content of the amino groups in the CS. Increasing temperature and strength of NaOH enhances the acetyl group removal from chitin, which then produces CS with different properties. CS was one of the main cationic polymers which forms inter and intra-molecular hydrogen bonding due to amine and hydroxyl groups which made the crystalline structure of CS rigid (Choi *et al*., 2016).

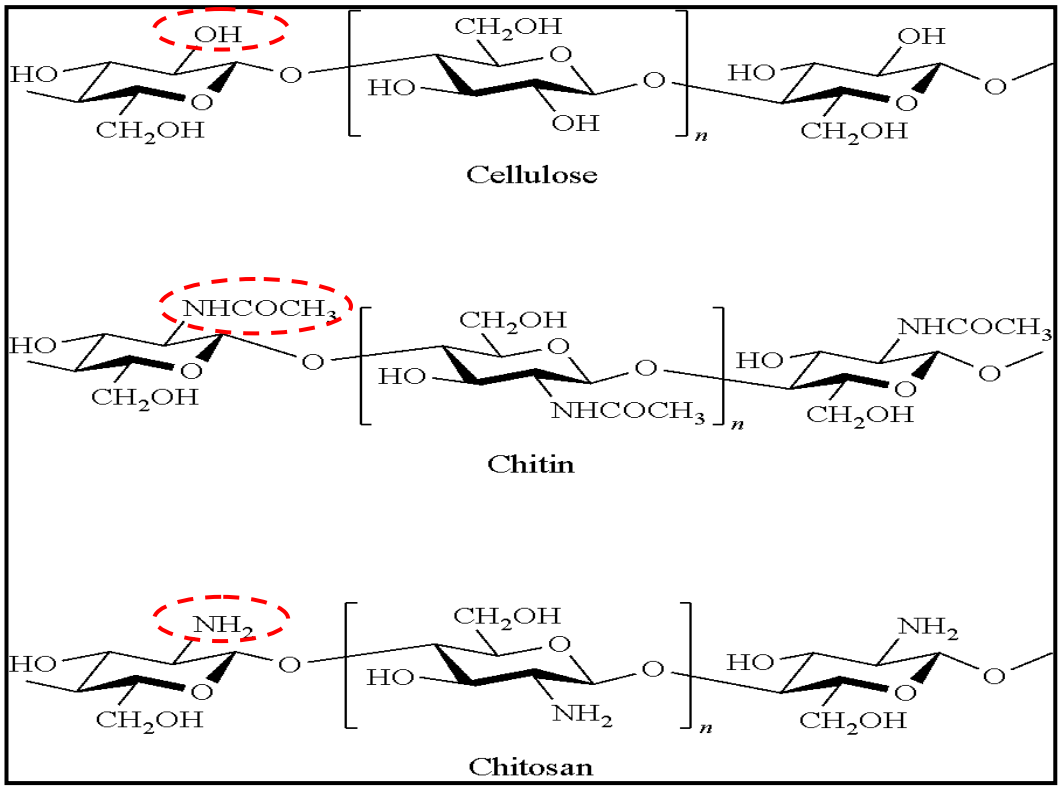

Figure 1.6: Molecular structures of cellulose, chitin and chitosan (Kirsch *et al*., 2014).

1.4.2 Applications of CS

CS is biodegradable, biocompatible, bioadhesive, hydrophilic, able to produce film and a good adsorbent (Zhao *et al*., 2015). The diverse properties of CS made it usable in different applications and fields such as pharmaceutical, biomedical, food, cosmetics (Rinaudo, 2006) and waste water remediation (Cárdenas *et al*., 2002; Janaki *et al*., 2012; Ngah and Fatinathan, 2010). The functionality of CS was based on the presence of hydroxyl and amino group which served as the coordination and reaction sites for modification which could attract the positive and negative chemical species to bound to its structure (Ngah and Fatinathan, 2010).

CS can also become bioadhesive since it offers a very good strength as compared to synthetic adhesive without containing volatile organic carbon (VOC)

(Patel, 2015). However, the material suffers from low strength and large shrinkage upon dehydration. Therefore, other materials such as clay when added into the CS matrix can significantly improve its thermal stability and mechanical properties, and may exert special behavior towards chemical species present in water (Wang *et al*., 2006). Such a system can also be used to fasten flocculation and improve the flake's textures (Shou *et al*., 2012).

1.4.3 Modification of CS

CS is not soluble in organic solvents and only dissolved in acidic aqueous media (HCl and CH_3COOH) whereby the solubility of CS is facilitated by the protonation of its primary amino group on the C-2 position of the D-glucosamine. The degree of protonation depends on the pKa of the acid and CS concentration which only converts CS into the pseudonatural cationic polymer (García *et al*., 2015; Rinaudo *et al*., 1999). Due to its excellent and vast properties, CS was modified chemically in order to produce novel CS-based materials or biohybrid with specific application properties which usually occurs at the $–NH_2$ primary group and hydroxyl group at the C-2 and C-6 position, respectively (García *et al*., 2015). However, due to its poor solubility in organic solvents, researchers have focused on improving its solubility and grafting process by attaching new functional groups. Garcia *et al*. (2015) had reported a novel and simple method via nitroxide-mediated polymerization (NMP) to modify well-defined molecular weight CS in homogeneous media by utilizing CS-sodium dodecylbenzenesulfonate (SDBS)-glycidyl methacrylate (GMA) as a precursor. The poly (styrene) (PS), poly (butyl acrylate) (PBA), poly (acrylic acid) (PAA) respectively, are grafted onto the hydroxyl groups of CS-SDBS-GMA in DMSO to produce CS-GMA-PS, CS-GMA-PBA and CS-GMA-PAA as new CS based materials. Cai *et al*. (2009) prepared the soluble CS in

DMSO by grafting organo-soluble polymers, poly (ethyleneglycol) (PEG) and poly (ε-caprolactone) (PCL) onto CS using the acidic CS and sodium dodecylsulfate (SDS) solution as an intermediate. The authors found that the PEG and PCL became conjugated to CS through the hydroxyl groups while maintaining the cationic density of the amino groups intact on the surface of the CS. The SDS and SDBS which were responsible for the dissolution of grafted CS in DMSO could be removed by precipitation of the grafted polymer in DMSO into Tris aqueous solution or dialyzing against Tris solution (Cai *et al*., 2009; García *et al*., 2015).

Meanwhile, the CS films, beads, gels and fibers which were prepared by single CS solution suffer dehydration shrinkage in aqueous media and swelling defects upon thermal treatment. In addition, the solubility of CS in acidic media can be cumbersome, which eventually decrease the spectrum of its application (Ngah *et al*., 2005). To overcome this, the CS was modified chemically by cross-linkers such as epichlorohydrin (ECH), glutaraldehyde (GLA), glyoxal, ethylene glygol diglycidyl ether (EDGE), tripolyphosphate (TPP) and genipin (Berger *et al*., 2004; Obeid *et al*., 2013) basically to change the hydrophilicity of CS to be more hydrophobic. The cross-linking occurs in the amine and hydroxyl groups in C-2 and C-6 position that allows the formation of bridges between the polymer chains. Among the cross-linking agents, the dialdehydes such as GLA and glyoxal bind preferentially to the amino group of CS forming covalent imine bonds via a Shiff reaction while the epoxides, such as ECH prefers to bind to the free hydroxyl group (Berger *et al*., 2004). The cross-linked CS has an improved mechanical resistance, strength and stability in acidic, alkaline and chemical solution as well as under thermal treatment and compression (Azlan *et al*., 2009; Ngah *et al*., 2002). However, cross-linking agents such as GLA is known to be neurotoxic while glyoxal is

mutagenic, which may not be a good choice for biomedical, medical, pharmaceutical and tissue engineering applications (Berger *et al*., 2004).

Recently, the attention has been devoted to modifying the CS structure by combining with other potential materials such as zeolite and MT. The hydrophilic CS forms composite with clays which are alumino-silicates with a three-dimensional framework structure containing AlO_4 and SiO_4. Such combination would avoid the use of toxic and mutagenic chemicals which can harm human health. In addition, the combination of the two different types of adsorbents could improve the pore size, mechanical strength, chemical stability, hydrophilicity and biocompability of CS (Ngah *et al*., 2012). Another approach in modification of CS was via photo irradiation which causes changes in the polymeric structure of CS by inducing the chain scission, reducing the average molecular weight, improving solubility in water, changing the color intensity, optical and spectral sensitivity (Taei, 2011). CS has been modified by different light sources such as UV light (Praxedes *et al*., 2012), fluorescent lamp (Jawad and Nawi, 2012b), ultrasonic irradiation (Cravotto *et al*., 2005; Kasaai *et al*., 2008) and gamma (γ) rays (Kang *et al*., 2007; Tahtat *et al*., 2012). Nevertheless, until recently, the oxidative degradation are based on the formation of reactive $^{\bullet}OH$ radicals from H_2O_2 (Chang *et al*., 2001), TiO_2 (Jawad and Nawi, 2012b) and O_3 (Yue *et al*., 2009) which are powerful oxidizing species. It receives attention whereby modification occurs when the oxidative radical species attack the 1,4 glycosidic linkages which result in the CS degradation (Kang *et al*., 2007). Modification of CS by a combination of photon from light source and oxidants could turn CS into the desired properties such as water-soluble, low molecular weight with added specialty in biological, chemical and physical properties than that of the ordinary CS (Kang *et al*., 2007).

1.5 Montmorillonite

1.5.1 Structure and properties

Montmorillonite (MT), the clay mineral is often confused with bentonite. Both bentonite and MT belong to the smectite group which is built from 2:1 aluminosilicate whereby alumina octahedral is switched between two tetrahedral of silica layers (Bhattacharyya and Gupta, 2008). In short, bentonite can be considered as the family name while MT is the species name. MT is referred to as "swelling clay minerals" due to the tendency for polar liquids to be taken in the interlayer space which makes MT a matrix for the preparation of functional composites in adsorbents, catalyst and flame retardants (Sun *et al*., 2015).

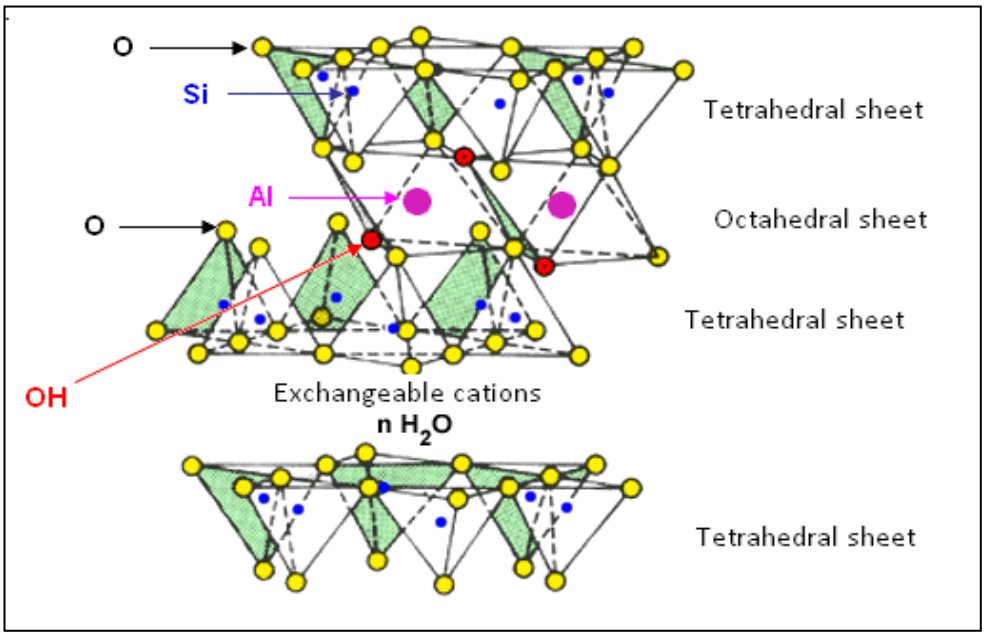

Figure 1.7: The structure of MT. Source: http://sparc.fpv.umb.sk/ (accessed on 9.10 pm, 21st Feb 2016).

The clay layer is characterized by permanent negative charges due to isomorphous substitution of Al^{3+} atoms of the octahedra for lower valent cations (Mg^{2+}). Exchangeable cations (Na^{+}) are present in the interlayer spaces to

compensate the negative charge. In addition to the permanent charge, pH-dependent charge is present on the edges of clay layer; Al–OH (or Si–OH) groups at the edges are present as different states depending on the pH of the solution: $Al–OH^{2+}$ (at low pH), Al–OH (at medium pH), and Al–O– (at high pH). Other than MT, there are several kinds of smectite-type clay minerals (e.g., saponite, hectorite, beidelite, and nontronite), which differ in chemical composition and the type of isomorphous substitution. Most of these clay minerals occur naturally in earth soils, whereas the composition, isomorphous substitution, impurity level, and crystallinity of the clays differ depending on the production areas. Synthetic clay minerals, which are suitable for chemical experiments due to lower impurity content, are also available (Nakato and Miyamoto, 2009).

1.5.2 Applications of MT in environmental remediation

The interlayer of MT contains negative charges which are counterbalanced by inorganic cations (e.g., Na^{+}, Ca^{2+}) and exchangeable for adsorption of cationic contaminants such as heavy metals, cationic dyes (methylene blue (MB), malachite green (MG)) and cationic surfactants (Zhu *et al*., 2014). Since MT adsorbs cationic surfactant, it can undergo ion-exchange with its negative charge counterpart which the modified MT often called organo-MT was produced. Eventually, the modification can promote the adsorption of anionic contaminants such as humic acid, methyl orange (MO), 2-naphthol and neutral pollutant such as phenol (Jiang *et al*., 2002). Beside organic pollutants, organo-clays can also adsorb heavy metals such as Cu^{2+} and Zn^{2+} (Lin, 2002), Cr (VI) (Krishna *et al*., 2000) and Ni^{2+} (Ijagbemi *et al*., 2009). The properties of clays specifically MT as good adsorbents are due to their high specific surface area, high chemical and mechanical stability, cheap and vastly available from nature. Thus, MT has the potential to be widely used in wastewater

treatment for removing many types of pollutants and heavy metals besides activated carbon, a universal but costly adsorbent which restricts its wide application (Zhu *et al*., 2014).

1.6 Conducting polymer: Polyaniline

The breakthrough discovery of intrinsically conducting polymer (ICP) was initiated by MacDiarmid, Heeger and Shirakawa in 1977 whereby they discovered the exposure of polyacetylene to iodine vapor yielding conducting material (MacDiarmid, 2001). ICPs are completely different form the conducting polymers which are merely a physical mixture of conducting material (eg; metal or carbon powder) and a nonconductive polymer. ICPs on the other hand, are commonly known as a "synthetic metal" which possess the electrical, electronic, magnetic and optical properties of a metal while retaining the mechanical properties and processability (MacDiarmid, 2001). Recently, ICPs discovered were polypyrrole (Ppy), polythiophene, polyparaphenylene (PPP) and polyparaphenylene vinylene (PPV) (Bhadra *et al*., 2009).

Polyaniline (PANI), known as "aniline black" was rediscovered in 1980s (Ćirić, 2013). PANI emerged as the promising material in the family of conducting polymers which allow the construction of polymer modified electrodes to be used as sensors, biosensors, and substrates for metallization (Ahmed, 2004). PANI has controlled conductivity within 10^{-10} – 10^{1} S cm^{-1} range with ionic and proton conductivity, redox activity, electro- and solvatochromism, electrical storage, stable in extreme condition, high thermal stability and easy to synthesize (Ahmed, 2004; Yu and Shishov, 2012). The synthesis of PANI has expanded over the years and it became the most studied conducting polymer. Under different conditions, PANI can

exist in three main oxidation states as shown in Figure 1.8. The oxidation states on the other hand, are denoted by the y values as shown in Figure 1.9 whereby y = 1, 0.5 and 0 corresponding to the fully reduced polyaniline (benzenoid diamine), the half oxidized polyaniline (emeraldine), and the fully oxidized polyaniline (quinoid diimine), respectively (Wang *et al*., 2013b). According to Bhadra *et al*. (2009), the mode of synthesis was varied which were based on chemical, electrochemical, template, enzymatic, plasma and photo approaches. The most common method, chemical approach can be subdivided into the following modes as shown in Table 1.2.

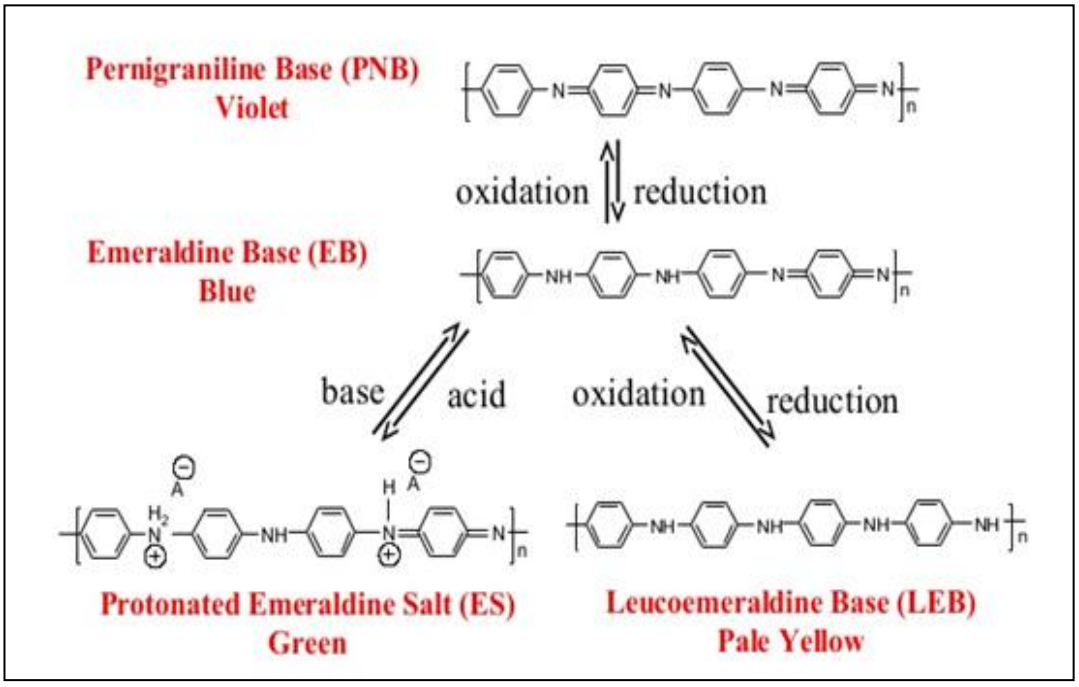

Figure 1.8: Structures of polyaniline in various intrinsic redox states (Chen, 2007)

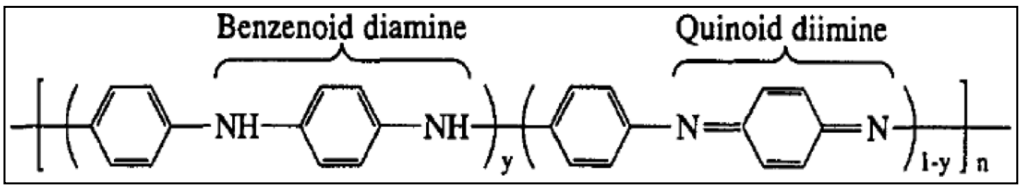

Figure 1.9: Molecular structure of emeraldine base of PANI (Zeng and Ko, 1998).

Table 1.2: Various methods for synthesization of PANI (Bhadra *et al*., 2009).

Method	Description
Heterophase	Polymerization includes the precipitation, suspension, micro suspension, emulsion, miniemulsion, microemulsion, dispersion, reverse micelle and inverse (Carenza and Palma, 1985)
Solution	Processability is better since the prepared PANI is already in a solution (Kuramoto and Tomita, 1997).
Interfacial	Polymerization is carried out in a mixture of two immiscible solvents such as water and chloroform in the presence of different acids as dopants (Chen *et al.*, 2007; Dallas *et al.*, 2007).
Seeding	A typical template approach whereby foreign material is used as a seed. PANI obtained is similar to a nanofiber with high conductivity which dependent on the type and concentration of acids, the type of seed, solvent and the relative amount of seed to solvent (Xing *et al*., 2006).
Metathesis	PANI is formed when *p*-dichlorobenzene and sodium amide is heated at 220 °C for 12 hours in an organic medium such as benzene, whereby aniline monomer is not required (Guo *et al*., 2005).
Self assembling	The PANI films are grown on the film by polymerizing an aniline monomer in a vapor phase (Yang *et al*., 2007)
Electrochemical	i) Constant current (galvanostatic) Two-electrode assembly dipped in an electrolyte solution containing monomer, with specified current (Genies *et al*., 1985) ii) A constant potential (potentiostatic) PANI powder adheres weakly on the electrode (Diaz and Logan, 1980). iii) A potential scanning/cycling or sweeping (Diaz and Logan, 1980).
Sonochemical	Dropwise addition of an acidic ammonium persulfate (APS) solution to an acidic aniline solution with the aid of ultrasonic irradiation. The possible reactions within the system are (Jing *et al*., 2007): i) the continuous formation of primary PANI nanofibers; ii) the conversion of primary nanofibers into thicker fibers with uneven surfaces; and iii) the growth and agglomeration of thicker.